AIP | Journal of Applied Physics

Manipulation of magnetization reversal of Ni81Fe19 nanoellipse arrays by tuning the shape anisotropy and the magnetostatic interactions

Y. Wang, W. H. Shi, H. X. Wei, D. Atkinson, B. S. Zhang, and X. F. Han

Citation: Journal of Applied Physics **111**, 07B909 (2012); doi: 10.1063/1.3676215
View online: http://dx.doi.org/10.1063/1.3676215
View Table of Contents: http://scitation.aip.org/content/aip/journal/jap/111/7?ver=pdfcov
Published by the AIP Publishing

Manipulation of magnetization reversal of $Ni_{81}Fe_{19}$ nanoellipse arrays by tuning the shape anisotropy and the magnetostatic interactions

Y. Wang,[1,2] W. H. Shi,[1] H. X. Wei,[2] D. Atkinson,[3] B. S. Zhang,[1] and X. F. Han[2,a)]
[1]*Nanofabrication Facility, Suzhou Institute of Nano-tech and Nano-bionics, Chinese Academy of Science, Suzhou 215125, China*
[2]*Beijing National Laboratory for Condensed Matter Physics, Institute of Physics, Chinese Academy of Science, Beijing 100190, China*
[3]*Durham University Physics Department, Rochester Building, Durham DH13LE, United Kingdom*

(Presented 3 November 2011; received 26 September 2011; accepted 9 November 2011; published online 5 March 2012)

Two series of highly ordered two-dimensional arrays of $Ni_{81}Fe_{19}$ nanoellipses were nanofabaricated with different aspect ratios, R, and element separations, S, to investigate the influence of the self-demagnetization and the magnetostatic interaction upon the magnetization reversal. For nanostructures with low shape anisotropy, an additional magnetic easy axis was induced orthogonal to the shape-induced easy axis by reducing the separations along both axes. For the structures with larger shape anisotropy, the switching field distribution/coercivity (SFD/H_c) was reduced, and for the array with the smallest separations (20 nm and 35 nm along the long and short axes, respectively), coherent rotation of the whole array occurred. The magnitude of both the shape anisotropy and a configurational anisotropy induced by the magnetostatic interactions have been estimated. These results provide some useful information for the design of potential magnetic nanodot logic and for high-density magnetic random access memory. © *2012 American Institute of Physics*. [doi:10.1063/1.3676215]

I. INTRODUCTION

Novel and emerging nanomagnetic and spintronic devices, such as magnetic logic gate (MLG)[1–3] and magnetic random access memory (MRAM),[4,5] have been extensively studied and are regarded as potential candidates for future information technology. The MLG concepts reported[1–3] rely upon magnetostatic interactions between adjacent single-domain nanomagnets to information transfer and logical processing. For high-density MRAM, "cross-talk" between neighboring cells due to magnetostatic interaction increases significantly as the memory density increases. To develop future MLG systems and high-density MRAM further, it is important to understand the influence of magnetostatic interactions upon the magnetization reversal behavior in densely packed arrays and in particular two-dimensional arrays. To obtain a suitable domain structure and maintain good thermal stability, elliptically shaped nanostructures have been commonly adopted, so in addition to array spacing, the influence of the shape-induced anisotropy also needs to be considered. However, most work has focused upon either two-dimensional isotropic circular dot arrays or chains of structures with vortex domain structures.[6,7] Far fewer studies have investigated arrays of ellipses or taken into account the shape anisotropy.[8–12] Webb and Atkinson[8] and Endo *et al.*[9] have separately reported that increased magnetostatic interactions along the long axis of chains of Ni–Fe nanoellipses enhance the coercivity. Lyle *et al.*[10] showed that in nanoscale elliptical magnetic tunnel junction structures, chains of structures parallel to the short axis of the ellipse develop a configurational anisotropy and overcome the inherent shape anisotropy to define a new easy axis direction. Jain *et al.*[11] and Yin *et al.*[12] have recently explored the competition between shape anisotropy and configurational anisotropy in linear chains; however, the results were complicated due to the complex multi-domain structures. Also, in these investigations, the shape anisotropy of the elliptical elements was kept constant, the magnetostatic interactions were significant only along the chains, and the interaction-induced easy axis dominated the original shape anisotropy.[10] Therefore, it remains necessary to systematically explore how the magnetization reversal of nanoscale elliptical elements are influenced by varying both the shape anisotropy and the magnetostatic interactions along both the short and long axes of the structures.

In this paper, we reported a systematic study of two-dimensional arrays of $Ni_{81}Fe_{19}$ nanoellipses with the element separations down to 20 nm. The results should be useful for the design of future MLG and high-density MRAM.

II. EXPERIMENTAL METHODS

Two series of two-dimensional arrays of nanoellipses were patterned on the same wafer by electron beam lithography and Ar^+ ion beam etching of a 20-nm-thick $Ni_{81}Fe_{19}$ film with 2-nm Ru caplayer deposited on Si/SiO_2 substrate by sputtering. The nanostructures in the two series of arrays had different aspect ratios, R (defined the ratio of the long axis, a, to short axis, b), of 1.5 and 2 but in both series the nanostructures had the same short axis dimensions, $b = 65$ nm. Figure 1(a) illustrates the element dimensions and array spacing. For the

a)Author to whom correspondence should be addressed. Electronic mail: xfhan@aphy.iphy.ac.cn.

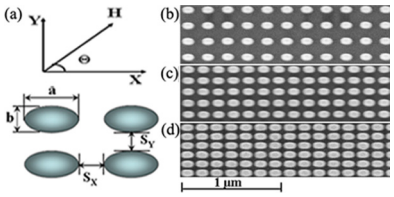

FIG. 1. (Color online) (a) The illustration for nanoellipse array, and the SEM images of arrays $R = 2$ with (b) $S_x = 85$ nm, and $S_y = 100$ nm, (c) $S_x = 35$ nm and $S_y = 50$ nm, and (d) $S_x = 20$ nm and $S_y = 35$ nm, respectively.

arrays of nanostructures with $R = 1.5$, the element separation was $S_{1x} = S_{1y}$, where S_{1x} ranged from 30 to 90 nm. For the arrays with $R = 2$, $S_{2x} = S_{2y}$-15 nm, where S_{2x} ranged from 20 to 85 nm. Figures 1(b)–1(d) show SEM images of the arrays of nanoellipses where $R = 2$. The uniformity of the shapes was good, and clearly defined edges were observed in all of the arrays down to the smallest separation, $S_{2x} = 20$ nm. The magnetization reversal was investigated at room temperature using a longitudinal magneto-optical Kerr effect (MOKE) system with focused laser spot of about 5 μm and the single-domain structure was confirmed by MFM measurement.

III. RESULTS AND DISCUSSION

Figure 2 shows the dependence of coercivity, H_c, upon separation measured at different field angles for the arrays of nanoellipses with $R = 1.5$. Thereinto, the angular dependence of the MOKE loops for the largest separations $S_{1x} = S_{1y} = 90$ nm is presented in the top-left inset of Fig. 2. The angle, θ, ranged from 0° to 90°, and represented the angle between the applied magnetic field, H, and the long axis of the nanoellipses (x direction). At $\theta = 90°$, the magnetization response was linear indicating hard axis magnetization behavior. The same measurements were performed for the arrays with separations $S_{1x} = S_{1y} = 40$ nm and $S_{1x} = S_{1y} = 30$ nm, respectively, and a similar angular dependence of the magnetization behavior was obtained. Here, for θ in the ranges from 0° to 60°, the coercivity increases non-linearly as the nanostructure separations (S_{1x} and S_{1y}) increase. In contrast, at $\theta = 90°$ (y direction), H_c falls with increasing separations. The bottom-right inset Fig. 2 shows the MOKE loops for $\theta = 0°$ and $\theta = 90°$ for the smallest array spacing ($S_{1x} = S_{1y} = 30$ nm). The effect of separation is clear, at $\theta = 90°$, the remanence ratio, M_r/M_s, is approximately zero for the widely spaced array ($S_{1x} = S_{1y} = 90$ nm) but rises to nearly 50% for the most closely spaced array ($S_{1x} = S_{1y} = 30$ nm). The variation of H_c at $\theta = 90°$ indicates that the initial shape-induced magnetic hard axis changes as a result of the competition between the self-demagnetization energy and the significantly increased magnetostatic interactions along both axes. However, the original shape-induced easy axis is maintained. Based upon previous theoretical work,[3] an additional easy axis can help initialize a MLG array, allowing accurate functional performance. Hence, this result may be useful for the design of future high-performance MLG.

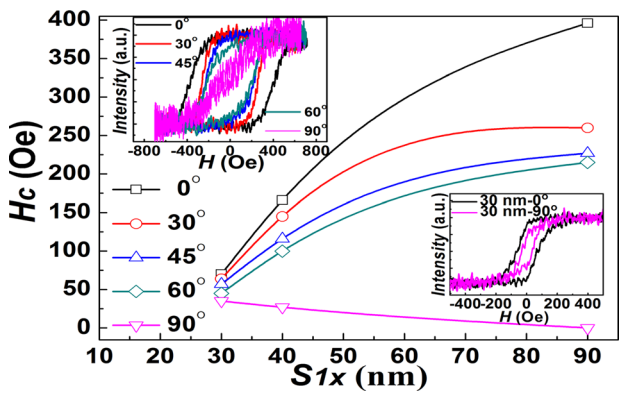

FIG. 2. (Color online) The dependence of coercivity (H_c) upon separations S_{1x} at different angles for the array $R = 1.5$ and the MOKE loops for array with the largest separation $S_{1x} = 90$ nm at different angles (top-left inset) and with $S_{1x} = 30$ nm at $\theta = 0°$ and 90°, (bottom-right inset) respectively.

Figure 3(a) shows the MOKE loops taken from arrays of structures with $R = 1.5$, at $\theta = 0°$, with separations S_{1x} ($= S_{1y}$) = 90, 40, and 30 nm, respectively. The shape of the MOKE loops change and H_c decreases significantly as the separations decrease. In contrast, recent work on one-dimensional chains of nanoellipses, showed that the coercivity increased as the separations decreased.[8,9] This highlights the difference between one- and two-dimensional magnetostatic interactions. To understand the influence of the magnetostatic interactions on the magnetization reversal in two-dimensional arrays of nanoellipses, the effective anisotropy constant, K_{eff}, the configurational anisotropy, K_{conf}, and the normalized switching field distribution (SFD/H_c) have been analyzed quantitatively. Because the magnetic nanoelliptical structures can be regarded as single domains, one can get $K_{\text{eff}} = \mu_0 H_k M_s/2$, where H_k represents the anisotropy field, and M_s is the saturation magnetization of $Ni_{81}Fe_{19}$, nominally 8.6×10^5 A/m. The demagnetization energy constant arising from the shape anisotropy is $K_d = \frac{1}{2}\mu_0(N_y - N_x)M_s$, where the N_y and N_x are the demagnetizing factors along y direction and x direction, respectively. According to previous results,[13] it is reasonable to assume that for the largest separations $S_{1y} = S_{1x} = 90$ nm there is only a very weak or even no

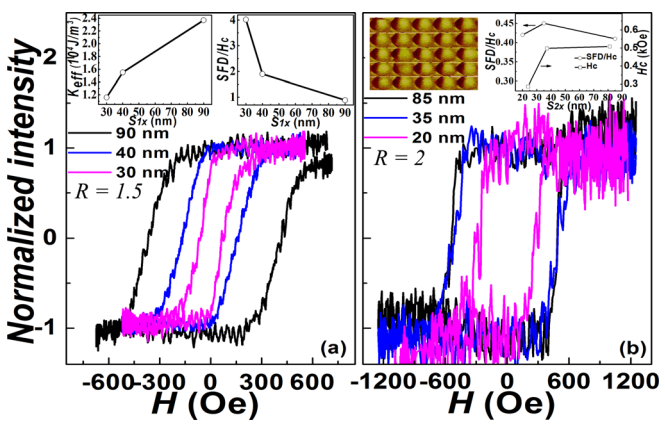

FIG. 3. (Color online) The MOKE loops taken from the arrays $R = 1.5$ with different separations S_{1x} ($= S_{1y}$) (a) and R = 2 with different separations S_{2x} (b) at $\theta = 0°$ and the deduced K_{eff} (top-left inset in (a)) and SFD/H_c (top-right inset in (a)) and the remanent state MFM imaging (top-left inset in (b)) and the SFD/Hc and Hc (top-right inset in (b)) as a function of corresponding separations.

magnetostatic interactions between the elements, so the total anisotropy can be attributed to the shape anisotropy. Hence, $K_{\text{eff}} = K_d$, and thus the inherent shape anisotropy constant is about 2.37×10^4 J/m^3 for $R = 1.5$. For medium or small separations of S_{1x} and S_{1y}, the magnetostatic interactions are taken into account $K_{\text{eff}} = K_d + K_{dipX} - K_{dipY}$, where the K_{dipX} (K_{dipY}) represents the magnetostatic energy along x (along y) direction and K_{dipX}-K_{dipY} is also called the configurational anisotropy K_{conf}. K_{eff} for the arrays with $S_{1x} = S_{1y} = 40$ nm and $S_{1x} = S_{1y} = 30$ nm is significantly lower at 1.55×10^4 J/m^3 and 1.16×10^4 J/m^3, respectively. The top-left inset of Fig. 3(a) shows the K_{eff} values as a function of separation S_{1x}. In addition, for each separation, the configurational anisotropy was estimated to be about 0 J/m^3, 0.82×10^4 J/m^3, and 1.21×10^4 J/m^3, respectively. The decrease of K_{eff} may be attributed to the contribution of the anisotropy K_{dipY} term along the y direction. It has been shown that if K_{dipY} is dominant, the effective anisotropy will be totally changed.[10] Therefore, it also suggests that the magnetostatic interaction along x is needed to maintain the original shape-defined easy axis orientation.

The normalized switching field distribution (SFD/H_c) for the arrays with weak shape anisotropy ($R = 1.5$) are plotted in the top-right inset of Fig. 3(a). The SFD/H_c ratios obtained here are too large and the magnetostatic interaction along the y direction too strong for the application of these arrays in high-density MRAM. The influence of the shape-induced anisotropy was investigated with arrays of nanoellipses with $R = 2$. Figure 3(b) shows the MOKE loops at $\theta = 0°$ for arrays of structures with $R = 2$ and separation $S_{2x} = S_{2y} - 15$ nm, where S_{2x} was 85, 35 and 20 nm, respectively. From these measurements, K_d was about 3.33×10^4 J/m^3 and the nanoellipses were observed to have a single-domain structure from remanent state MFM imaging, as shown in the top-left inset of Fig. 3(b). Interestingly, for two arrays with separations $S_{2x} = 85$ nm, $S_{2y} = 100$ nm and $S_{2x} = 35$ nm, $S_{2y} = 50$ nm, the MOKE loops and H_c values are similar, even though strong magnetostatic interaction exists only in the latter array. From this, the $K_{dipX} = K_{dipY}$ can be deduced. While for the array with $S_{2x} = 20$ nm and $S_{2y} = 35$ nm, the sharp decrease in H_c indicates that $K_{dipY} > K_{dipX}$. Moreover, according to the report of Kirk *et al.*,[13] magnetostatic interactions along the short axis of the nanostuctures will broaden the switching field distribution. Here, all the arrays of structures with $R = 1.5$ (top-right inset of Fig. 3(a)) and most of the arrays with $R = 2$ (top-right inset of Fig. 3(b)) are consistent with this observation. The exception is for the case of $R = 2$ with $S_{2x} = 20$ nm and $S_{2y} = 35$ nm, where the SFD/H_c decreases notably even though the magnetostatic interactions along y direction are much stronger than along x direction. One reason for this may be that, in this array of the nanostructures, they are so strongly coupled that they switch as a coherent array. The SFD/H_c was reduced by increasing the aspect ratio of the nanoellipses to $R = 2$, and to minimize the magnetostatic interactions, S_y should be at least larger than 50 nm and S_y should also be larger than S_x. These results may serve as a guide for the design of high-density MRAM.

IV. CONCLUSIONS

In summary, by tuning both the shape anisotropy and configurational anisotropy, the magnetization reversal of the two-dimensional arrays of $Ni_{81}Fe_{19}$ nanoellipses can be controlled. For the low aspect ratio ellipses ($R = 1.5$), a further magnetic easy axis can be induced, while the original easy axis orientation is maintained. This should be beneficial for future high-performance MLG. For the arrays with higher aspect ratio ellipses ($R = 2$), the switching field distrbution (SFD/H_c) can be reduced. This is highly relevant to applications in MRAM technology. Furthermore, to avoid the "cross-talk" in MRAM, spacing, S_y, should be at least larger than 50 nm and S_y should be larger than x-axis spacing, S_x. Analysis indicates that the K_{conf} (along y) will lower the array barrier energy and decrease H_c. These results provide some useful guidance for the further applications of MLG and MRAM based on arrays of nanoscale elliptical structures.

ACKNOWLEDGMENTS

The project was supported by the State Key Project of Fundamental Research of the Ministry of Science and Technology (MOST, No. 2010CB934400) and the National Natural Science Foundation of China (NSFC, Grant Nos. 10934099, 10874225, and 51021061), the UK Royal Society, and the partial support of the Graduate Education Project of Beijing Municipal Commission of Education and K. C. Wong Education Foundation, Hong Kong.

[1]R. P. Cowburn, and M. E. Welland, Science **287**, 1466 (2000).
[2]A. Imre, G. Csaba, L. Ji, A. Orlov, G. H. Bernstein, and W. Porod, Science **311**, 205 (2006).
[3]L. Gross, R. R. Schlittler, G. Meyer, and R. Allenspach, Nanotechnology **21**, 325301 (2010).
[4]S. S. P. Parkin, K. P. Roche, M. G. Samant, P. M. Rice, R. B. Beyers, J. Appl. Phys. **85**, 5828 (1999).
[5]S. Tehrani, J. M. Slaughter, E. Chen, M. Durlam, J. Shi, and M. DeHerrera, IEEE Trans. Magn. **35**, 2814 (1999).
[6]V. Novosad, K. Yu. Guslienko, H. Shima, Y. Otani, S. G. Kim, K. Fukamichi, N. Kikuchi, O. Kitakami, and Y. Shimada, Phys. Rev. B **65**, 060402(R) (2002).
[7]M. Natali, A. Popa, U. Ebels, Y. Chen, S. Li, and M. E. Welland, J. Appl. Phys. **96**, 4334 (2004).
[8]J. L. Webb, and D. Atkinson, J. Appl. Phys. **103**, 033905 (2008).
[9]Y. Endo, H. Fujimoto, Y. Kawamura, R. Nakatani, and M. Yamamoto, IEEE Trans. Magn. **44**, 2718 (2008).
[10]A. Lyle, A. Klemm, J. Harms, Y. Zhang, H. Zhao, and J. P. Wang, Appl. Phys. Lett. **98**, 092502 (2011).
[11]S. Jain, A. O. Adeyeye, and N. Singh, Nanotechnology **21**, 285702 (2010).
[12]X. L. Yin, S. H. Liou, A. O. Adeyeye, S. Jain, and B. S. Han, J. Appl. Phys. **109**, 07D354 (2011).
[13]K. J. Kirk, J. N. Chapman, S. McVitie, P. R. Aitchison, and C. D. W. Wilkinson, Appl. Phys. Lett. **75**, 3683 (1999).